Supporting information for

Targeting the Hsp90 C-terminal domain by the chemically accessible dihydropyrimidinone scaffold

Maria Strocchia,‡[a] Stefania Terracciano,‡[a] Maria G. Chini,[a] Antonio Vassallo,[b] Maria C. Vaccaro,[a] Fabrizio Dal Piaz,[a] Antonietta Leone,[a] Raffaele Riccio,[a] Ines Bruno[a]* and Giuseppe Bifulco[a]*

[a]Department of Pharmacy, University of Salerno, via Giovanni Paolo II, 132, 84084, Fisciano, Italy. Fax: +39 089 969602; Tel: +39 089 969741; Tel: +39 089 969743 E-mail: bifulco@unisa.it; brunoin@unisa.it

[b] Department of Science, University of Basilicata, Viale dell'Ateneo Lucano n.10, 85100 Potenza, Italy

‡ These authors contributed equally to this work

1. General information

All commercially available starting materials were purchased from Sigma-Aldrich and were used as received. All solvents used for the synthesis were of HPLC grade; they were purchased from Sigma-Aldrich and Carlo Erba Reagenti. All NMR spectra (^{1}H, HMBC, HSQC) were recorded on a Bruker Avance 600 MHz instruments. All compounds were dissolved in 0.5 mL of 99.95% $CDCl_3$ (Carlo Erba, 99.95 Atom % D). Coupling constants (*J*) are reported in Herz, and chemical shifts are expressed in parts per million (ppm) on the delta (δ) scale relative to $CHCl_3$ (7.26 ppm for ^{1}H and 77.2 ppm for ^{13}C) as internal reference. Electrospray mass spectrometry (ESI-MS) was performed on a LCQ DECA TermoQuest (San Josè, California, USA) mass spectrometer.

Reactions were monitored on silica gel 60 F_{254} plates (Merck) and the spots were visualized under UV light. Analytical and semi-preparative reversed-phase HPLC was performed on Agilent Technologies 1200 Series high performance liquid chromatography using a Jupiter Proteo C_{18} reversed-phase column (250 x 4.60mm, 4μ, 90 Å, flow rate = 1 mL/min; 250 x 10.00mm, 10μ, 90 Å, flow rate = 4 mL/min respectively, Phenomenex®). The binary solvent system (A/B) was as follows: 0.1% TFA in water (A) and 0.1% TFA in CH_3CN (B). The absorbance was detected at 280 nm.The purity of all tested compound (>98%) was determined by HPLC analysis.

All microwave irradiation experiments were carried out in a dedicated CEM-Discover® Focused Microwave Synthesis apparatus, operating with continuous irradiation power from 0 to 300 W utilizing the standard absorbance level of 300 W maximum power. The reactions were carried out in 10 mL sealed microwave glass vials. The Discover™ system also offers controllable ramp time, hold time (reaction time) and uniform stirring. The temperature was monitored using the CEM-Discover built-in-vertically-focused IR temperature sensor. After the irradiation period, the reaction vessel was cooled rapidly (60-120 s) to ambient temperature by air jet cooling.

2. General procedure for Microwave-assisted Biginelli reaction.

A mixture of appropriate aldehyde (1.0 mmol), urea or its derivatives (1.5 mmol), 1,3-dicarbonyl compound (1.0 mmol) in acetonitrile (1.5 mL) was placed in a 10 mL microwave glass vial equipped with a small magnetic stirring bar. TMSCl (1.0 mmol) was added and the mixture was then stirred under microwave irradiation at 120°C for 15-20 min(Scheme S1).

Only in a few cases, TMSCl (procedure **a**) was replaced by 10 mol % $Yb(OTf)_3$ (procedure **b**) or $FeCl_3$ (procedure **c**) as Lewis acid catalysts, as needed. After irradiation, the reaction mixture was cooled to ambient temperature by air jet cooling, cold water was added and the vial was poured into crushed ice and then at 4°C overnight. The resulting precipitate was filtered and washed with a cold mixture of ethanol/water (1:1) (3x3 mL), to give the desired product in good yields (60-90%). HPLC purification was performed by semi-preparative reversed-phase HPLC (on a Jupiter Proteo C_{18} column: 250 x 10.00mm, 10μ, 90 Å, flow rate = 4 mL/min) using the gradient conditions reported below for each compound. The final products were obtained with high purity (>95%) as detected by HPLC analysis and were fully characterized by ESMS and NMR spectra.

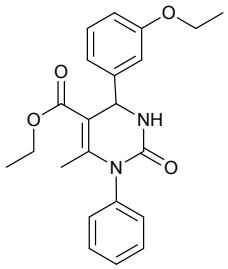

Compound **1** was obtained by following the general procedure **a** as a yellow gelatinous solid (110.0 mg, 73% yield). RP-HPLC t_R = 30.6 min, gradient condition: from 5% B to 100% B in 45 min, flow rate of 4 mL/min, λ= 280 nm. ^{1}H NMR (600 MHz, $CDCl_3$): δ = 1.21 (t, *J* = 7.1 Hz, 3H), 1.42 (t, *J* = 6.9 Hz, 3H), 2.10 (s, 3H), 4.03 (q, *J* = 7.0 Hz, 2H), 4.15 (q, *J* = 7.1 Hz, 2H), 5.46 (s, 1H), 6.84 (dd, *J* = 8.2, 2.1 Hz, 1H), 6.93 (s, 1H) 6.95 (d, *J* = 7.6 Hz, 1H), 7.25-7.29 (m, 2H), 7.41-745 (m, 4H); ^{13}C NMR (150 MHz, $CDCl_3$): δ = 14.9, 15.1, 19.0, 54.5, 60.5, 64.4, 112.5, 114.2, 115.1, 118.3, 117.9, 129.2, 129.5, 130.1, 131.3, 141.7, 145.1, 148.2, 158.2, 161.2, 168.4. ESMS, calcd for $C_{22}H_{24}N_2O_4$ 380.4; found m/z = 381.8 $[M + H]^+$.

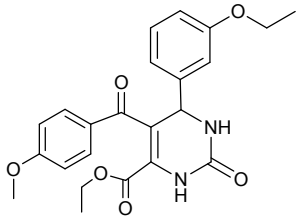

Compound **2** was obtained by following the general procedure **a**.

All analytical and spectral data were in accord with previously published data.[1]

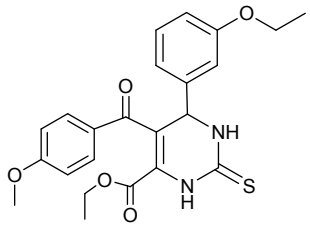

Compound **3** was obtained by following the general procedure **a** as a yellow powder (103.3 mg, 78% yield). RP-HPLC t_R = 31.8 min, gradient condition: from 5% B to 35% B in 10 min, increased to 100 % B in 65 min, flow rate of 4 mL/min, λ= 280 nm. ^{1}H NMR (600 MHz, $CDCl_3$): δ = 0.84 (t, *J* = 7.1 Hz, 3H), 1.33 (t, *J* = 6.9 Hz, 3H), 3.82 (s, 3H), 3.85-3.97 (m, 4H), 5.41 (s, 1H), 6.70 (s, 1H), 6.78 (d, *J* = 8.5 Hz, 3H), 7.16 (t, *J* = 7.9 Hz, 1H), 7.38 (br s, 1H), 7.58 (d, *J* = 8.6 Hz, 2H);^{13}C NMR (150 MHz, $CDCl_3$):δ = 13.2, 14.5, 56.7, 55.9, 56.3, 59.8, 113.4, 113.8, 114.2, 119.6, 119.9, 120.5, 130.9, 131.5, 131.8, 144.7, 159.7, 165.5, 180.1, 192.3. ESMS, calcd for $C_{23}H_{24}N_2O_5S$ 440.5; found m/z = 441.2 $[M + H]^+$.

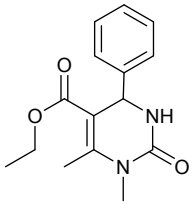

Compound **4** was obtained by following the general procedure **a** as a yellow gelatinous solid (135.7 mg, 89% yield). RP-HPLC t_R = 23.6 min, gradient condition: from 5% B to 30% B in 10 min, increased to 90 % B in 50 min, flow rate of 4 mL/min, λ= 280 nm. All spectral data were in accord with previously published data.[2]

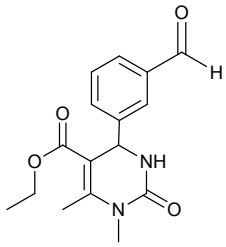

Compound **5** was obtained by following the general procedure **b** as a yellow gelatinous solid (62.9 mg, 60% yield). RP-HPLC t_R = 23.9 min, gradient condition: from 5% B to 25% B in 10 min, increased to 95 % B in 50 min, flow rate of 4 mL/min, λ= 280 nm. ^{1}H NMR (600 MHz, $CDCl_3$): δ = 1.18 (t, *J* = 7.1 Hz, 3H), 2.53 (s, 3H), 3.26 (s, 3H), 4.10 (q, *J* = 7.1 Hz, 2H), 5.45 (s, 1H), 7.47-7.55 (m, 2H),7.77 (br s, 2H), 9.98 (s, 1H);^{13}C NMR (150 MHz, $CDCl_3$): δ = 14.3, 19.0, 30.3, 54.1, 61.0, 105.9, 129.9, 130.3, 132.5, 137.8, 143.6, 147.9, 156.7, 166.4, 192.1. ESMS, calcd for $C_{16}H_{18}N_2O_4$ 302.3; found m/z = 303.1 $[M + H]^+$.

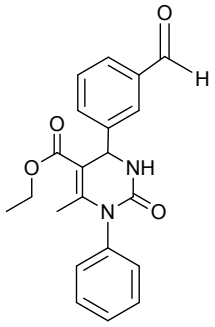

Compound **6** was obtained by following the general procedure **c** as a pale orange gelatinous solid (124.4 mg, 62% yield). RP-HPLC t_R = 27.3 min, gradient condition: from 5% B to 100% B in 40 min, flow rate of 4 mL/min, λ= 280 nm. ^{1}H NMR (600 MHz, $CDCl_3$): δ = 1.19 (t, *J* = 7.1 Hz, 3H), 2.14 (s, 3H), 4.13 (q, *J* = 7.1 Hz, 2H), 5.59 (s, 1H), 7.30 (br s, 1H), 7.42-7.51 (m, 4H), 7.58 (t, *J* = 7.9 Hz, 1H), 7.71 (d, *J* =7.6 Hz, 1H), 7.86 (d, *J* = 7.4 Hz, 1H), 10.05 (s, 1H);^{13}C NMR (150 MHz, $CDCl_3$): δ = 14.7, 19.2, 54.8, 60.4, 106.8, 120.6, 124.0, 127.7, 130.4, 132.8, 138.1, 140.9, 141.7, 145.1, 148.2, 158.2, 168.4, 192.4. ESMS, calcd for $C_{21}H_{20}N_2O_4$ 364.4; found m/z = 365.3 $[M + H]^+$.

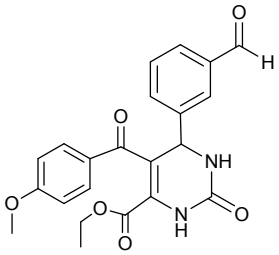

Compound **7** was obtained by following the general procedure **a**. All analytical and spectral data were in accord with previously published data.[1]

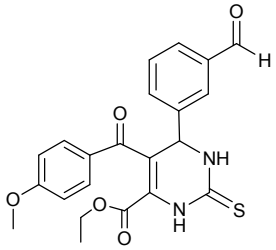

Compound **8** was obtained by following the general procedure **a** as a yellow powder (144.6 mg, 85% yield). RP-HPLC t_R = 28.3 min, gradient condition: from 5% B to 25% B in 10 min, increased to 90 % B in 50 min, flow rate of 4 mL/min, λ= 280 nm. ^{1}H NMR (600 MHz, $CDCl_3$): δ = 0.85 (t, *J* = 7.1 Hz, 3H), 3.82 (s, 3H), 3.92-4.03 (m, 2H), 5.53 (s, 1H), 6.79 (d, *J* = 8.8 Hz, 2H), 7.33 (br s, 1H), 7.44-7.54 (m, 2H), 7.60 (d, *J* = 8.7 Hz, 1H), 7.71 (s, 1H), 7.78 (d, *J* = 7.3 Hz, 1H), 9.91 (s, 1H);^{13}C NMR (150 MHz, $CDCl_3$): δ = 13.5, 54.8, 57.4, 61.9, 112.5, 113.6, 128.7, 129.0, 130.7, 131.4, 132.1, 133.5, 159.8, 165.6, 180.3, 190.8, 192.6. ESMS, calcd for $C_{22}H_{20}N_2O_5S$ 424.5; found m/z = 425.2 $[M + H]^+$.

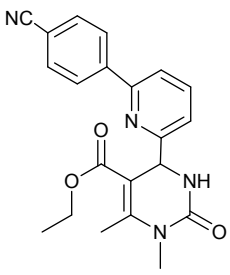

Compound **9** was obtained by following the general procedure **a** as a yellow gelatinous solid (112.0 mg, 90% yield). RP-HPLC t_R = 21.5 min, gradient

condition: from 5% B to 40% B in 10 min, increased to 100 % B in 50 min, flow rate of 4 mL/min, λ= 280 nm. ^{1}H NMR (600 MHz, $CDCl_3$): δ = 1.24 (t, *J* = 7.1 Hz, 3H), 2.51 (s, 3H), 3.22 (s, 3H), 4.18 (q, *J* = 7.0 Hz, 2H), 5.50 (s, 1H), 7.22 (d, *J* = 7.5 Hz, 1H), 7.67 (d, *J* = 7.7 Hz, 1H), 7.71-7.76 (m, 3H), 8.11 (d, *J* = 7.0 Hz, 2H); ^{13}C NMR (150 MHz, $CDCl_3$): δ = 14.4, 16.6, 30.4, 54.6, 60.4, 103.7, 119.6, 119.9, 120.9, 122.3, 127.4, 132.7, 138.1, 143.7, 151.3, 155.9, 162.8, 166.5. ESMS, calcd for $C_{21}H_{20}N_4O_3$ 376.4; found m/z = 377.1 $[M + H]^+$.

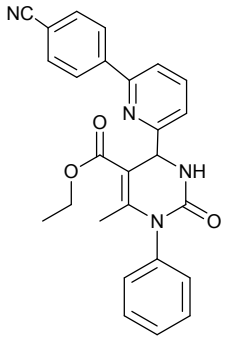

Compound **10** was obtained by following the general procedure **a** as a brownish gelatinous solid (177.4 mg, 67% yield). RP-HPLC t_R = 31.2 min**,** gradient condition: from 5% B to 35% B in 10 min, increased to 100 % B in 45 min, flow rate of 4 mL/min, λ= 280 nm. ^{1}H NMR (600 MHz, $CDCl_3$): δ = 1.27 (t, *J* = 7.1 Hz, 3H), 2.07 (s, 3H), 4.22 (q, *J* = 7.0 Hz, 2H), 5.66 (s, 1H), 6.99 (br s, 1H), 7.33-7.42 (m, 4H), 7.67-7.77 (m, 4H), 7.81(d, *J* = 7.5 Hz, 1H), 8.08 (d, *J* = 8.2 Hz, 1H);^{13}C NMR (150 MHz, $CDCl_3$): δ = 14.4, 16.6, 54.6, 60.4, 103.7, 119.6, 119.9, 120.9, 122.3, 127.4, 129.3, 130.0, 132.7, 138.1, 141.6, 143.7, 151.3, 155.9, 162.8, 166.5. ESMS, calcd for $C_{26}H_{22}N_4O_3$ 438.5; found m/z = 439.1 $[M + H]^+$.

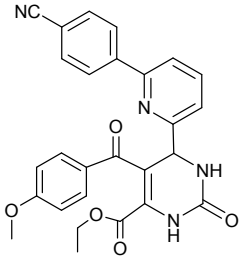

Compound **11** was obtained by following the general procedure **a**.

All analytical and spectral data were in accord with previously published data.[1]

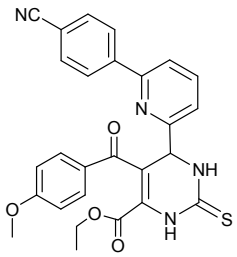

Compound **12** was obtained by following the general procedure **a** as a red gelatinous solid (70.3 mg, 70% yield). RP-HPLC t_R = 30.0 min, gradient condition: from 5% B to 100% B in 45min, flow rate of 4 mL/min, λ= 280 nm.

^{1}H NMR (600 MHz, $CDCl_3$): δ = 0.85 (t, *J* = 7.1 Hz, 3H), 3.78 (s, 3H), 3.89-4.00 (m, 2H), 5.62 (s, 1H), 6.72 (d, *J* = 8.7 Hz, 2H), 7.33 (br s, 1H), 7.61-7.70 (m, 5H), 7.81 (br s, 1H), 7.87 (d, *J* = 8.3 Hz, 2H); ^{13}C NMR (150 MHz, $CDCl_3$):δ = 13.8, 55.4, 59.9, 62.7, 113.4, 114.1, 119.5, 120.3, 120.5, 122.4, 127.2, 127.6, 129.8, 131.5, 141.4, 143.6, 151.6, 155.8, 159.5, 163.0, 165.7, 192.3. ESMS, calcd for $C_{27}H_{22}N_4O_4S$ 498.6; found m/z = 499.4 $[M + H]^+$.

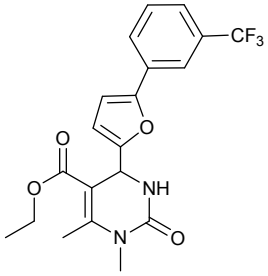

Compound **13** was obtained by following the general procedure **a**.

All analytical and spectral data were in accord with previously published data.[1]

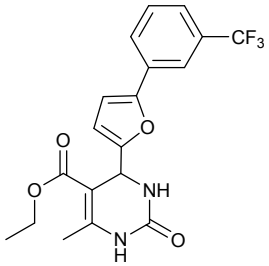

Compound **14** was obtained by following the general procedure **a** as a brownish gelatinous solid (75.6 mg, 78% yield). RP-HPLC t_R = 25.6 min, gradient condition: from 5% B to 40% B in 10 min, increased to 100 % B in 50 min, flow rate of 4 mL/min, λ= 280 nm. ^{1}H NMR (600 MHz, $CDCl_3$): δ = 1.24 (t, *J* = 7.1 Hz, 3H), 2.37 (s, 3H), 4.17 (q, *J* = 7.0 Hz, 2H), 5.56 (s, 1H), 6.22 (d, *J* = 3.3 Hz, 1H), 6.59 (d, *J* = 3.3 Hz, 1H), 7.43-7.51 (m, 2H), 7.73 (br s, 1H), 7.81 (s, 1H); ^{13}C NMR (150 MHz, $CDCl_3$):δ = 13.7, 14.8, 56.0, 60.2, 102.9, 108.0, 110.8, 123.7, 127.4, 128.6, 130.3, 133.5, 136.4, 151.6, 155.4, 156.0, 166.8. ESMS, calcd for $C_{19}H_{17}F_3N_2O_4$ 394.3; found m/z = 395.1 $[M + H]^+$.

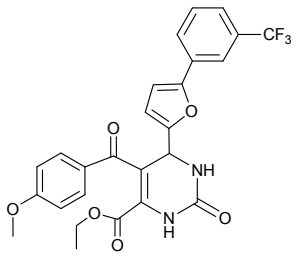

Compound **15** was obtained by following the general procedure **a**.

All analytical and spectral data were in accord with previously published data.[1]

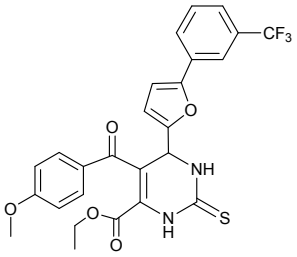

Compound **16** was obtained by following the general procedure **a**.

All analytical and spectral data were in accord with previously published data.[1]

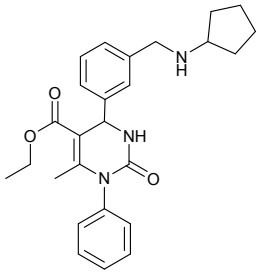

Compound **17** was obtained from compound **6** by reductive amination with cyclopentylamine as a yellow powder (33.8 mg, 90% yield). RP-HPLC t_R = 19.5 min**,** gradient condition: from 5% B to 100% B in 45 min, flow rate of 4 mL/min, λ= 280 nm. ^{1}H NMR (600 MHz, $CDCl_3$): δ = 1.16 (t, J = 7.1 Hz, 3H), 1.49 (br s, 2H), 1.62-1.77 (m, 4H), 1.9 (br s, 2H), 3.30 (s, 1H), 3.88 (s, 2H), 4.05-4.13 (m, 2H), 5.45 (s, 1H), 6.88 (br s,1H), 7.16 (br s, 1H), 7.29-7.35 (m, 3H), 7.37-7.44 (m, 3H), 7.47 (s, 1H); ^{13}C NMR (150 MHz, $CDCl_3$): δ = 14.5, 18.9, 23.9, 29.8, 50.3, 53.9, 58.7,60.8, 108.4, 126.8, 129.4, 129.8, 130.6, 139.2, 144.2, 150.5, 156.2, 166.4. ESMS, calcd for $C_{26}H_{31}N_3O_3$ 433.55; found m/z = 434.3 $[M + H]^+$.

3.Surface Plasmon Resonance Analyses

Recombinant human Hsp90α was purchased from Abcam (Abcam, Cambridge, UK). Proteomic grade trypsin was purchased from Sigma-Aldrich (Sigma-Aldrich Co, St Louis, MO, USA). The Hsp90 inhibitor 17-(Allylamino)-17-demethoxygeldanamycin (17-AAG) was purchased from Sigma-Aldrich.

SPR analyses were carried out according to our previously published procedures.[3-5] Briefly, SPR analyses were performed using a Biacore 3000 optical biosensor equipped with research-grade CM5 sensor chips (GE Healthcare). Using this platform, two separate recombinant Hsp90α surfaces, a BSA surface and one unmodified reference surface were prepared for simultaneous analyses.

Proteins (100 μg mL^{-1} in 10 mM CH_3COONa, pH 5.0) were immobilized on individual sensor chip surfaces at a flow rate of 5 μL min^{-1} using standard amine-coupling protocols to obtain densities of 8–12 kRU.

Compounds **1**-**17**, as well as 17-AAG, were dissolved in 100% DMSO to obtain 4 mM solutions, and diluted 1:200 (v/v) in PBS (10 mM NaH_2PO_4, 150 mM NaCl, pH 7.4) to a final DMSO concentration of 0.5%. Compounds concentration series were prepared as twofold dilutions into running buffer: for each sample, the complete binding study was performed using a six-point concentration series, typically spanning 0.025–1 μM, and triplicate aliquots of each compound concentration were dispensed into disposable vials. Binding experiments were performed at 25°C, using a flow rate of 50 μL min^{-1}, with 60 s monitoring of association and 300 s monitoring of dissociation (Table S1).

Simple interactions were suitably fitted to a single-site bimolecular interaction model (A+B = AB), yielding a single K_D. Sensorgram elaborations were performed using the BIAevaluation software provided by GE Healthcare.

Table S1. Thermodynamic constants measured by SPR for the interaction between tested compounds and immobilized Hsp90α.

Compound	K_D (μM)
1	0.0756±0.0071
2	0.0137±0.0017
3	No Binding
4	No Binding
5	No Binding
6	3.860±0.331
7	0.176±0.0089
8	0.3626±0.0289
9	No Binding
10	No Binding
11	No Binding
12	1.1475±0.098
13	No Binding
14	No Binding
15	No Binding
16	No Binding
17	0.0295±0.0014
17-AAG	0.388±0.089

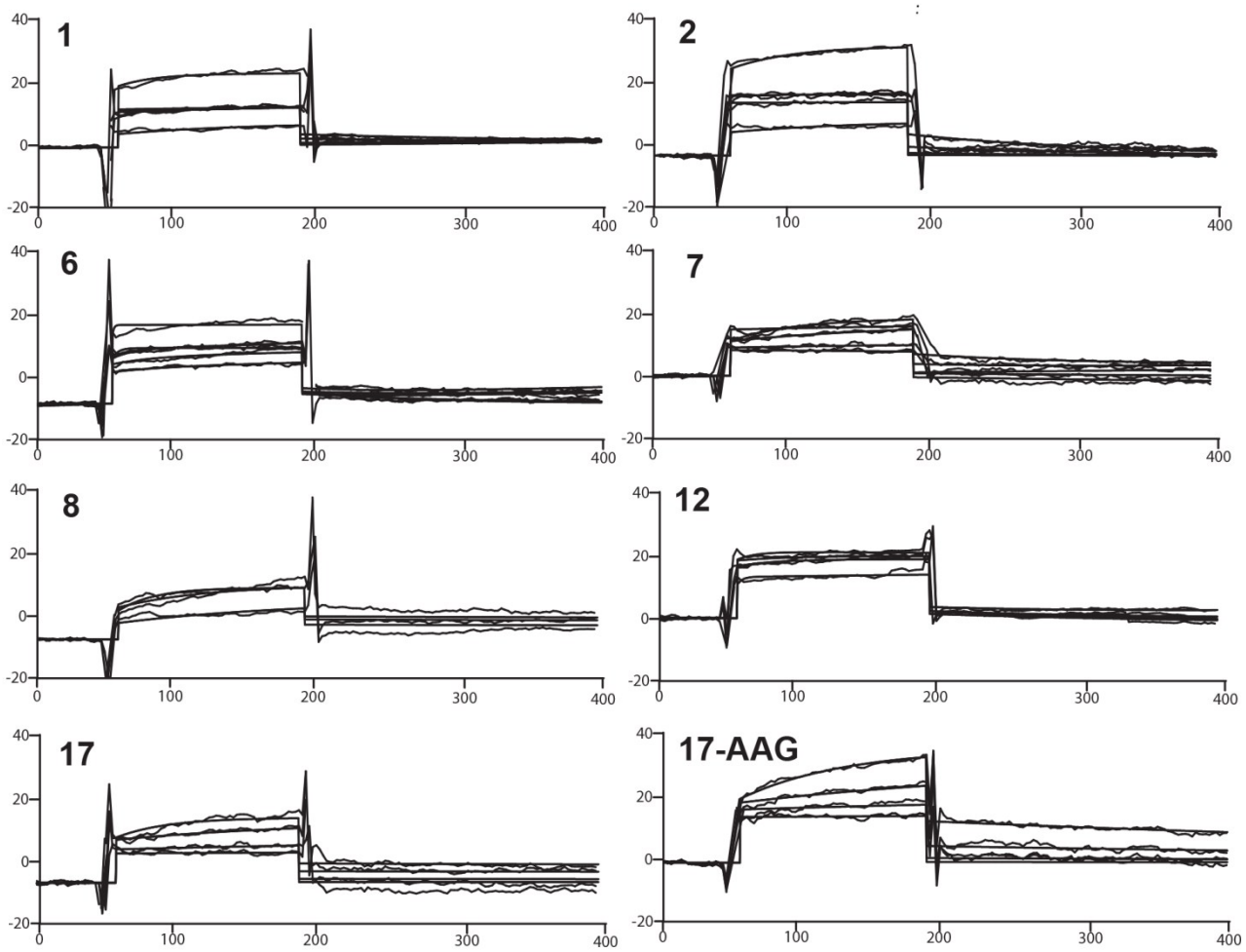

Fig. S1 Surface Plasmon Resonance sensorgrams acquired for compounds interacting with Hsp90α and for the positive control 17-AAG. Each compound was injected onto an Hsp90α modified sensor chip at 6 different concentrations in the range 0.025–1 μM.

4. Antiproliferative studies

Anti-Hsp70 (Abcam, Cambrige,UK); anti-Hsp90α/ß (H-114) sc-7947, anti-Raf1 (C-12): sc-133, anti-pAkt, antibodies were purchased from Santa Cruz Biotechnology (Santa Cruz Biotechnology, Inc., Delaware, CA, USA); anti-Akt was purchased from Cell Signaling (Cell Signaling Technology Inc., Beverly, MA, USA); anti-actin antibody was purchased from Sigma-Aldrich.

4.1 Cell culture and treatment

A375 (human melanoma) and Jurkat (human leukemic T-lymphocyte) cells, obtained from Cell Bank in GMP-IST (Genova, Italy) were cultured in Dulbecco's modified Eagle medium (DMEM)

or RPMI 1640 medium, respectively, supplemented with 10% (v/v) FBS, 2mM l−glutamine and antibiotics (100 U/mL penicillin, 100 µg/mL streptomycin) purchased from Invitrogen (Carslbad, CA, USA), at 37°C in humidified atmosphere with 5% CO_2. To ensure logarithmic growth, cells were subcultured every 2 days. As control cells, human peripheral blood mononuclear cells (PBMC) were isolated from buffy coats of healthy donors (kindly provided by the Blood Center of the Hospital of Battipaglia, Salerno, Italy) by using standard Ficoll−Hypaque gradients. Freshly isolated PBMC contained 92.8 ± 3.1% live cells. Proliferation of PBMC was induced by phytohemagglutinin (PHA) (10 µg mL^{-1}). Stock solutions of compounds **1**, **2**, **6**, **7**, **8**, **12**, **17** (100 mM in DMSO) were stored at 4°C in the dark and diluted just before addition to the sterile culture medium. In all the experiments, final concentration of DMSO was 0.15% (v/v).

4.2 Cell proliferation and viability

A375 ($1x10^4$ /well) and Jurkat ($2x10^4$ /well) cells were seeded in triplicate in 96 well−plates and incubated for the 24 h in the absence or presence of different concentrations of compounds **1**, **2**, **6**, **7**, **8**, **12**, **17** (concentration between 10 µM to 150 µM) or 17-AAG (between 1 µM to 10 µM).
The number of viable cells was determined by using a [3-4,5-dimethyldiazol-2-yl]-2,5-diphenyl tetrazolium bromide (MTT, Sigma-Aldrich) conversion assay, according to the method described by Mosmann.[6] Briefly, following the treatment, 25 µL of MTT (5mg/mL in PBS) was added and the cells were incubated for additional 3 h at 37°C. Thereafter, cells were lysed and suspended with 100 µL of buffer containing 50% (v/v) N,N-dimethylformamide, 20% SDS (pH 4.5). The absorbance was measured with a microplate reader (Titertek multiskan MCC7340, LabSystems, Vienna, VA, USA) equipped with a 620 nm filter. The cell population growth inhibition was also tested by cytometric counting (trypan blu exclusion). IC_{50} values were calculated from cell viability dose−response curves and defined as the concentration resulting in 50% inhibition of cell survival, compared to control cells treated with DMSO. PBMC were treated with **1** used at the concentrations

corresponding to the IC_{50} values of A375 and Jurkat cells (50 μM or 20 μM, respectively) to evaluate their effects on non-cancer cells viability.

5. Western Blot analysis

The A375 and Jurkat cells were incubated for 24 h with compound **1** used at the concentrations corresponding to the IC_{50} values (50 or 20 μM). Treated cells were harvested and disrupted by freeze−thawing in RIPA buffer (50 mM Hepes, 10 mM EDTA, 150 mM NaCl, 1% NP-40, 0.5% sodium deoxycholate, 0.1% SDS, pH 7.4), supplemented with protease inhibitors cocktail (Sigma-Aldrich). Cell debris was removed by centrifugation at 4°C and the supernatant protein concentration was determined, according to the Bio-Rad Protein assay (Biorad Laboratories, CA, USA). Total proteins (30 μg) were separated by SDS-PAGE under denatured reducing conditions and were then transferred to nitrocellulose membranes. After blocking with 3% BSA, the membranes were incubated at 4°C overnight with the different primary antibodies diluted 1:1000: Anti-Hsp70 (Abcam, Cambrige,UK); anti-Hsp90α/ß, anti-Raf1, anti-pAkt, (Santa Cruz Biotechnology, Inc., Delaware, CA, USA); anti-Akt (Cell Signaling Technology Inc., Beverly, MA, USA); anti-actin antibody was purchased from Sigma-Aldrich.

After washing, the membranes were incubated at room temperature (1 h), with an appropriate peroxidase-conjugate secondary antibody. The bound antibodies were detected by enhanced chemiluminescence reagent (ECL, Rockford, USA), according to the manufacturer's instructions. Quantitative densitometry analyses were performed using a Gel Doc 2000 system (Biorad Laboratories, CA, USA).

6. Cell cycle distribution analysis

Cell DNA content was measured by propidium iodide (PI) incorporation into permeabilized cells, as described by Nicoletti et al. Briefly, the cells were cultured for 24 h in the presence of DMSO, compound **1** or 17-AAG at the concentrations corresponding to the IC_{50} values. After treatment, the

cells were washed with cold PBS and incubated with a PI solution (0.1% sodium citrate, 0.1% Triton X-100 and 50 μg/ml of prodium iodide, Sigma-Aldrich, 10 μg/ml Rnase A) for 30 min at room temperature. Data from 10.000 events for each sample were collected by a FACScalibur flow cytometry (Becton Dickinson, San Josè, CA) and cellular debris was excluded from analysis by raising the forward scatter threshold. Percentage of cells in the sub G_0/G_1 phase, apoptotic fraction, was quantified using the CellQuest software (Becton Dickinson). The distribution of cells in G_0/G_1, S, G_2/M phases was determined using ModFit LT cell cycle analysis software (Becton Dickinson). Results were expressed as a mean ± SD of three experiments performed in duplicate.

7. Limited Proteolysis

Limited proteolysis experiments[7-9] were performed on recombinant Hsp90α at 37°C, PBS 0.1% DMSO, using trypsin or chymotrypsin as proteolytic agents; 30 mL of a 3 μM Hsp90α solution were used for each experiment. Binary complex Hsp90α/**1** was formed by incubating the protein with a 5:1 molar excess of **1** at 37°C for 15 min prior to proteolytic enzyme addition. Both Hsp90α and Hsp90α/**1**complex were digested using a 1:100 (w/w) enzyme to substrate ratio. The extent of the reactions was monitored on a time-course basis by sampling the incubation mixture after 5, 15, and 30 min of digestion. Samples were analyzed by MALDI-TOF/MS using a MALDI micro MX (Waters). Mass data were elaborated using the Masslynx software (Waters). Preferential hydrolysis sites on Hsp90α under different conditions were identified on the basis of the fragments released during enzymatic digestion.

8. Effect of compound 1 on Hsp90α oligomerization

The ability of compounds **1** to affect Hsp90α oligomerization was assessed by chemical cross-linking, using bis-sulfosuccinimidyl suberate (BS3) (Pierce chemical, Rockford, IL), an amine-reactive cross-linker. Recombinant human Hsp90α was diluted in PBS to a final concentration of 2 μM. Stock solutions of 3 mM BS3 were freshly prepared before diluting to the final assay

concentration. The protein was treated with 0,25 mM of compound **1** dissolved in DMSO or with DMSO and incubated on ice for 1 h, prior to chemical crosslinking. Cross-linking with 25 μM BS3 was carried out at room temperature for 1 h. Each reaction mixture was then boiled in the presence of 4X sample buffer, was subjected to SDS-PAGE and was stained with the standard silver nitrate protocol (Fig. S2).

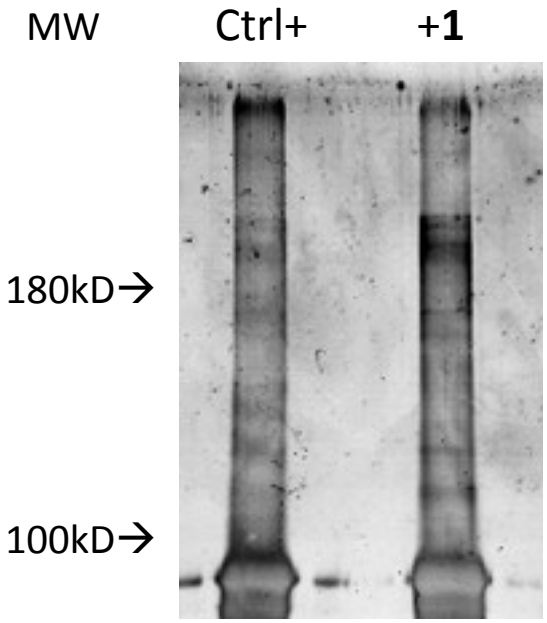

Fig. S2 Inhibition of Hsp90α oligomerization by compound **1**.

9. Statistical analysis

All the reported data represent the mean ± standard deviation (SD) of at least two independent experiments, performed in triplicate. Where necessary, data were statistically compared by Student's t-test; the statistical significance of DNA content between cells group was examined in the two-way analysis of variance (ANOVA) with Bonferroni post-test analysis using GraphPad Prism 5 software. Differences were considered significant if $p< 0.05$.

10. Molecular docking studies

The compound chemical structures (**1**-**17**) were processed with LigPrep (version 2.8)[10] generating all the possible tautomers and protonation states at a pH of 7.4 ± 1.0, and finally minimized using

OPLS 2005 force field. Protein 3D model was prepared using the Schrödinger Protein Preparation Wizard,[10] using the ATP-bound active state of ATP-bound active state of yeast Hsp82, an Hsp90α homologue (PDB code: 2CG9)[11] as model receptor. Docking calculations were performed using Glide software[10,12] with precision SP and XP. For all the compounds, all open-chain bonds were treated as active torsional bonds.

The binding site at the interface between chain A and B covering the C-terminal domain was explored during the docking calculations with an inner box of 12×12×12 Å, an outer box of 32×32×32 Å, and centered at -39.000 (x), 3.755 (y), and -9.714 (z). Default settings, except for the number of structures to save (10 in this case), were used for the docking studies. Post docking minimization was performed to optimize the ligand geometries. Results and illustrations of the 3D and 2D models were generated with VMD[13] and Maestro (version 9.6) software.

For the analysis of our docking studies, we have used the model obtained by Colombo et al.,[14] where the most frequent residues interacting with inhibitors are represented by Arg591, Asp503, Lys423, Gln596, and Arg599 of chain B, and Lys594 and Glu477 of chain A (Hsp90 residue numbering as in the PDB entry 2CG9).[11] On these bases, we have obtained the following 2D diagram interactions of **1**-**17** with the Hsp90 C-terminal domain (Fig. S3-S8).

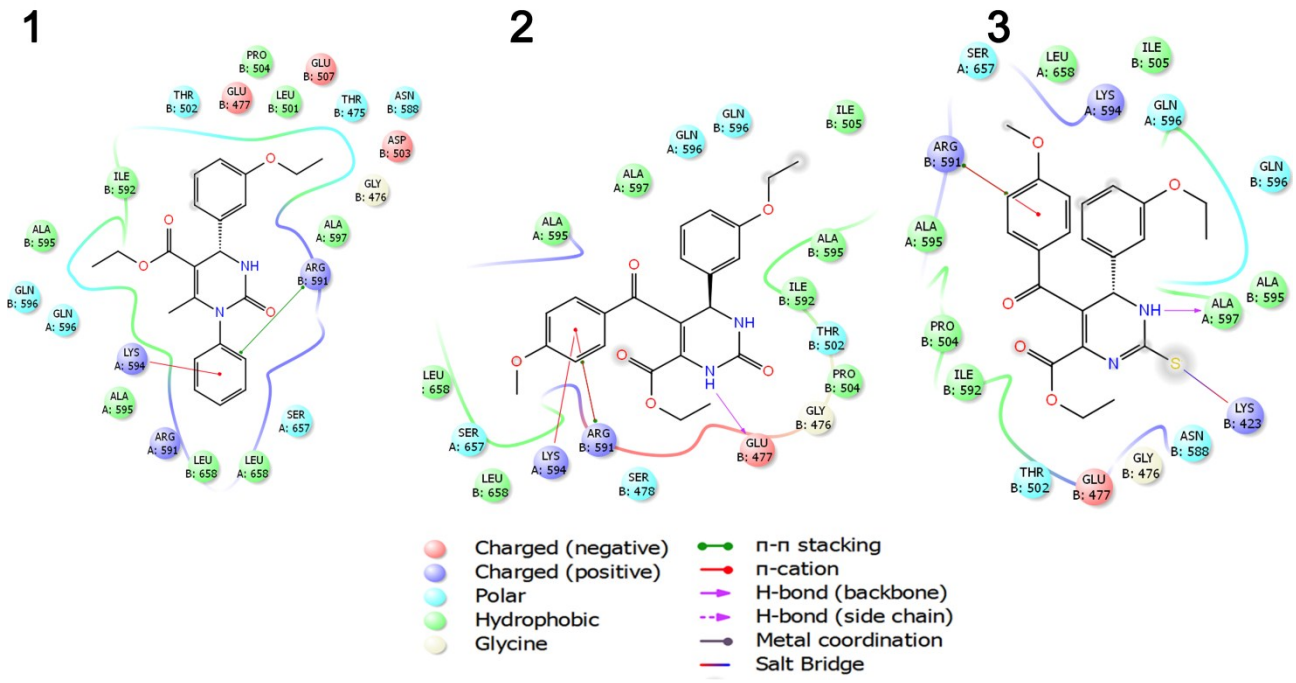

Fig. S3 2D diagram interactions of **1-3** with C-terminal domain of yeast Hsp90α (PDB: 2CG9).

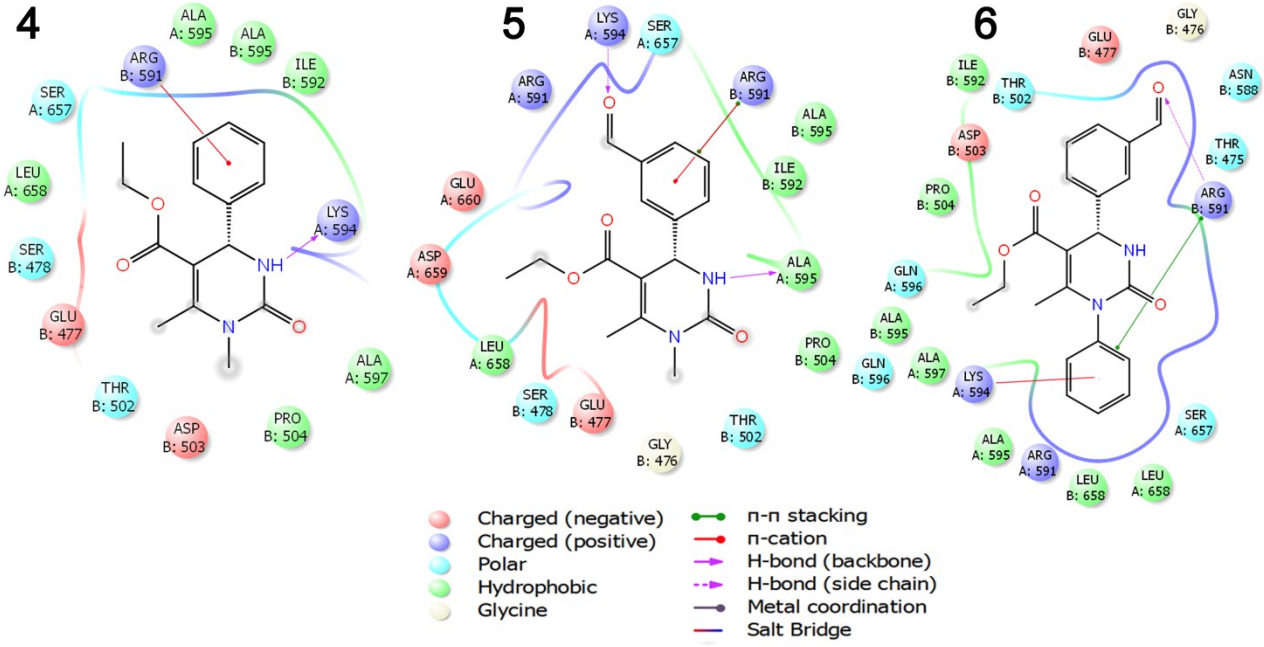

Fig. S4 2D diagram interactions of **4-6**with C-terminal domain of yeast Hsp90α (PDB: 2CG9).

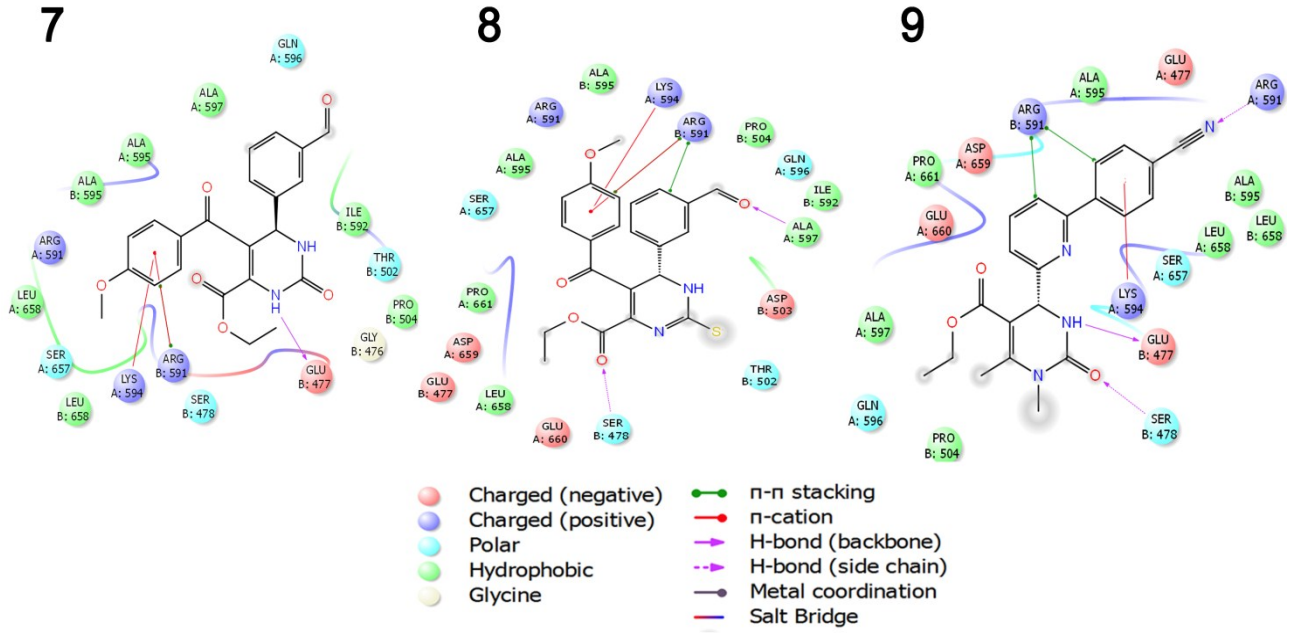

Fig. S5 2D diagram interactions of **7-9** with C-terminal domain of yeast Hsp90α (PDB: 2CG9).

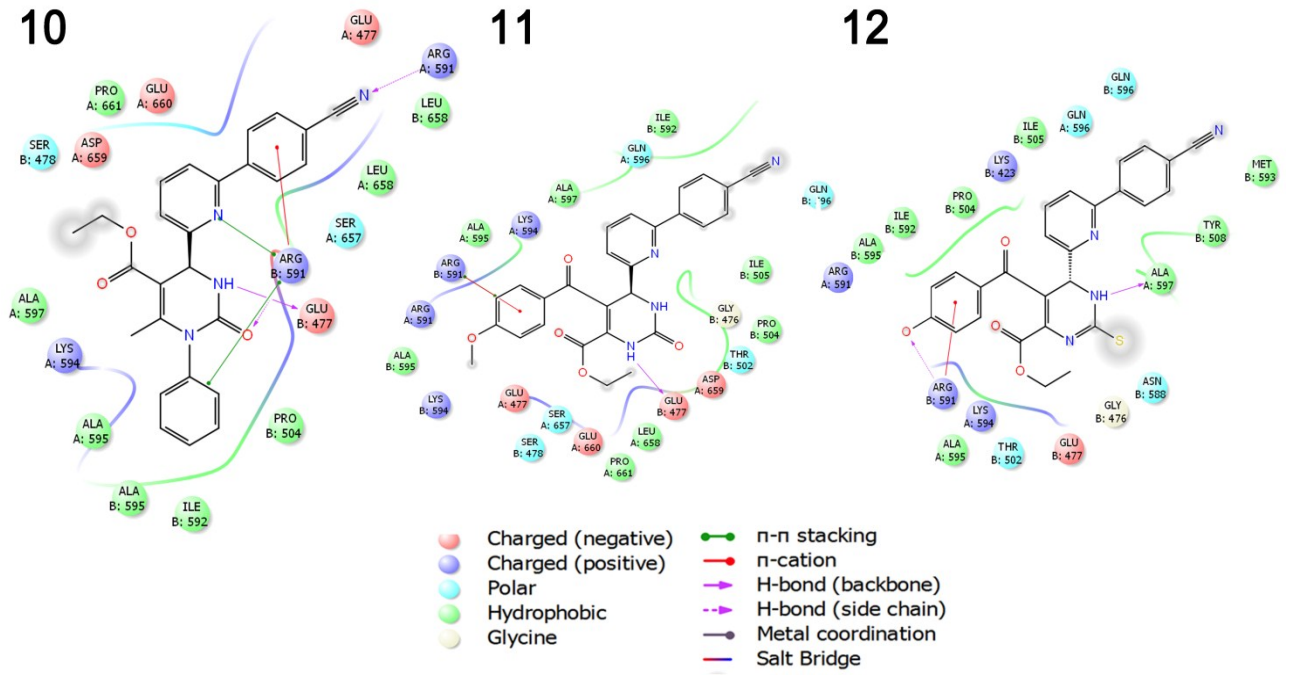

Fig. S6 2D diagram interactions of **10-12** with C-terminal domain of yeast Hsp90α (PDB: 2CG9).

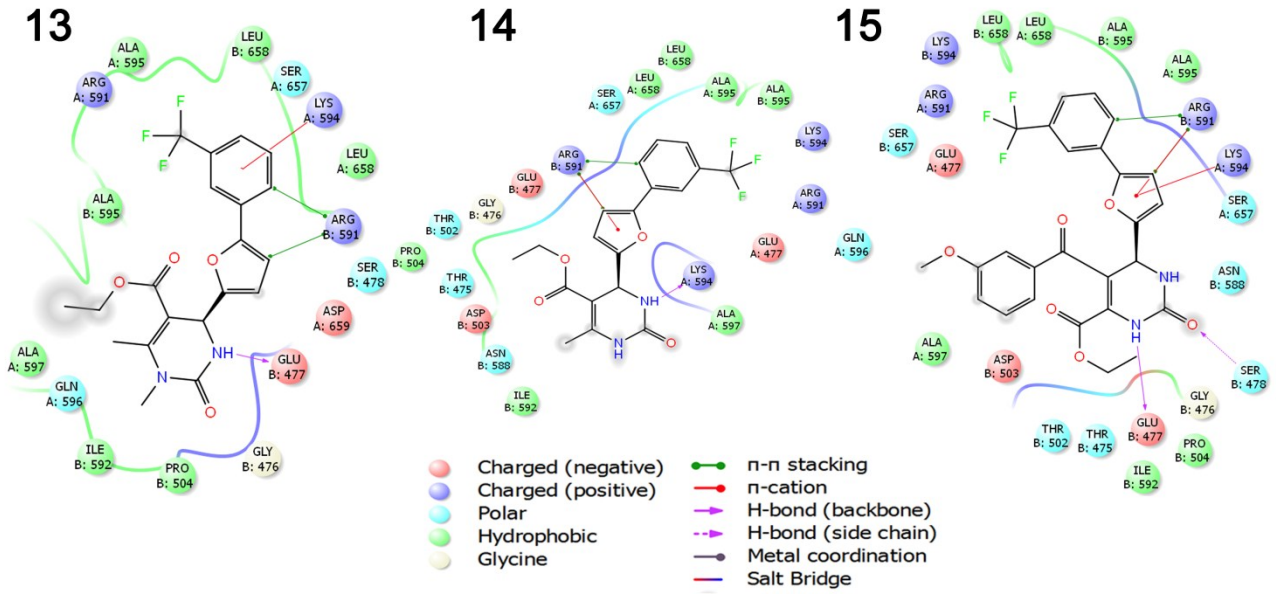

Fig. S7 2D diagram interactions of **13-15** with C-terminal domain of yeast Hsp90α (PDB: 2CG9).

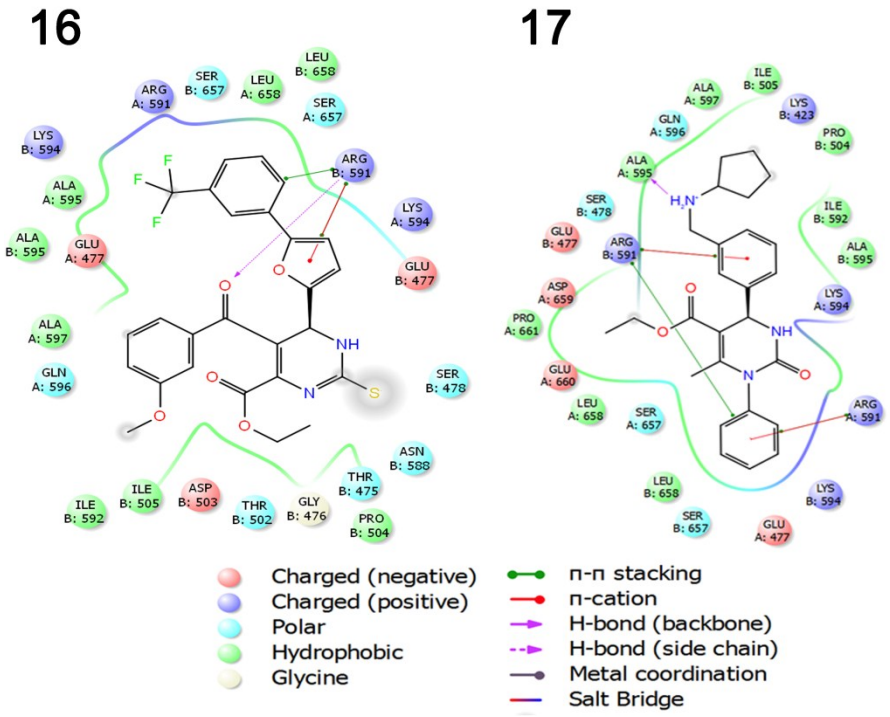

Fig. S8 2D diagram interactions of **16-17** with C-terminal domain of yeast Hsp90α (PDB: 2CG9).

The analysis of our models outlines the fundamental role of the substitution of the N-1 of the dihydropyrimidinone scaffold with a phenyl ring able to establish a double π-cation stacking interaction with Arg591 of chain B and Lys594 of chain A, and the simultaneous presence of a not bulky aldehydic portion at position 4 (see **1**, **6**, **17** vs **13-15**, Fig. S3, S4, S7 and S8). In fact, the compounds that show the presence of bulky (**13-16**, Fig S7-S8) or not substituted aldehyde (**4-5**, Fig

S4) at position 4 are completely inactive. On the other hand, the predicted activity slightly decreases when two aromatic rings are both present at R_2 and R_3 (such as for **7** and **8,** Fig. S5).

Starting from these considerations, we have performed the ADME Properties Prediction by using Qikprop[10] to explain the different activity on cell lines for **1**-**17**. In Table S2, we have reported the most representative properties, and among them, we have focused our attention on the calculated predicted apparent Caco-2 cell permeabilities (nm/sec).[15,16] We have used this calculated parameter to rationalize the different behavior of **1** with respect to the related compound **6** which contains the 3-formylphenyl group instead of the 3-ethoxypenyl at R_2 (Fig. S9).

Table S2. Properties of Tested Compounds Calculated by QikProp.[10]

Compound	mol MW[a]	QPPCaco2[b]	metab[c]	RuleOfFive[d]	rtvFG[e]	QPlogPo/w[f]	QPlogS[g]
1	380.4	1444.6	4	1	1	4.28	-5.33
2	424.5	538.0	4	0	2	2.98	-4.56
3	440.5	1572.8	5	1	3	5.21	-6.59
4	274.3	1012.5	3	0	1	3.33	-4.39
5	302.3	244.1	3	0	1	5.07	-6.54
6	364.4	344.6	3	0	1	3.67	-5.36
7	408.4	88.1	3	0	2	5.38	-6.37
8	424.5	295.7	4	0	3	3.88	-6.59
9	376.4	204.1	3	0	1	6.00	-6.94
10	438.5	232.3	3	1	1	5.32	-7.17
11	482.5	71.0	3	0	2	3.60	-6.58
12	498.6	340.2	4	0	3	5.00	-8.00
13	408.4	936.7	4	1	1	2.20	-3.49
14	394.4	566.0	4	1	1	3.81	-5.67
15	514.5	261.9	4	2	1	4.94	-7.64
16	530.5	1289.1	5	2	2	5.15	-6.32
17	433.5	241.0	5	1	1	5.10	-6.88

[a] Molecular weight, range 95% of drugs (130/725). [b] Caco2 cell permeability in nm/s, range 95% of drugs (<25 poor, >500 great). [c] Number of primary metabolites, range 95% of drugs (1/8). [d] Number of violations of Lipinski's rule of five.[17] The rules are: mol_MW < 500, QPlogPo/w < 5, donor HB ≤5, accptHB ≤10. Compounds that satisfy these rules are considered drug like. (The "five" refers to the limits, which are multiples of 5). [e] Number of reactive functional groups, range 95% of drugs (0 – 2). [f] Log of the octanol/water partition coefficient, range 95% of drugs (2/6.5). [g] Log of aqueous solubility S (mol/L), range 95% of drugs (-6.5/0.5).

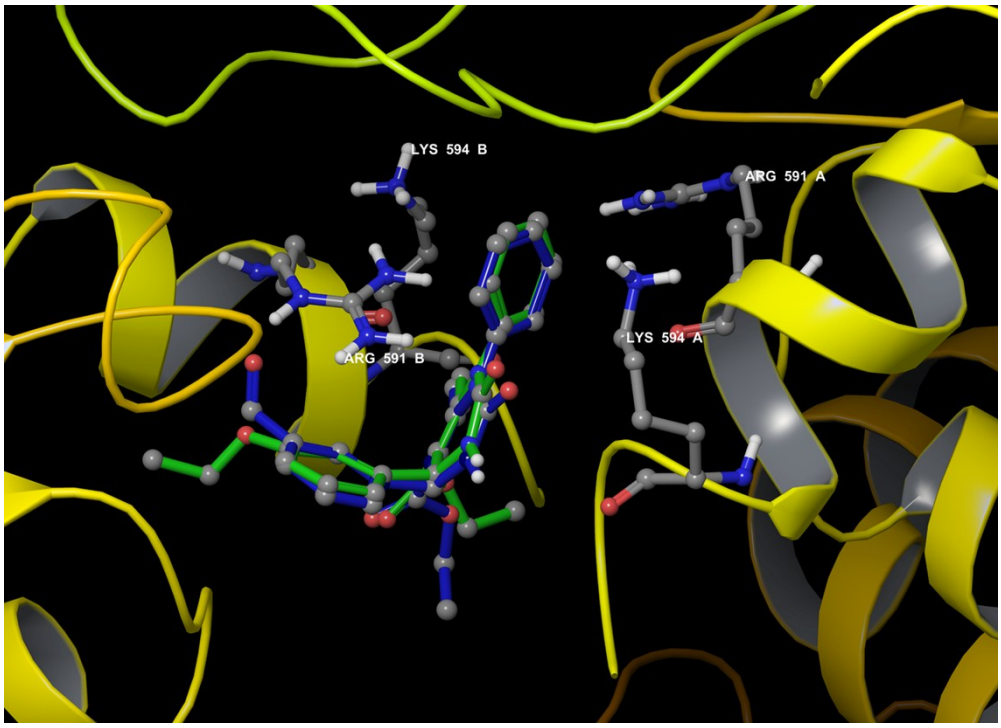

Fig. S9 Superimposition of **1** (green sticks) and **6** (blue sticks) in the C-terminal domain of of yeast Hsp90α.

References

1 G. Lauro, M. Strocchia, S. Terracciano, I. Bruno, K. Fischer, C. Pergola, O. Werz, R. Riccio and G. Bifulco, *Eur. J. Med. Chem.*, 2014, **10**, 407.

2 K. Singh, D. Arora, E. Poremsky, J. Lowery and R. S. Moreland, *Eur. J. Med. Chem.*, 2009, **44**, 1997.

3 A. Vassallo, M. C. Vaccaro, N. De Tommasi, F. Dal Piaz and A. Leone, *Plos One*, 2013, **8**, e74266.

4 F. Dal Piaz, A. Vassallo, L. Lepore, A. Tosco, A. Bader and N. De Tommasi, *J. Med. Chem.*, 2009, **52**, 3814.

5 S. Terracciano, M. G. Chini, F. Dal Piaz, A. Vassallo, R. Riccio, I. Bruno and G. Bifulco, *Eur. J. Med. Chem.*, 2013, **65**, 464.

6 T. Mosmann, *J. Immunol, Methods*, 1983, **65**, 55.

7 S. Orrù, F. Dal Piaz, A. Casbarra, G. Biasiol, R. De Francesco, C. Steinkühler and P. Pucci, *Protein Sci.*, 1999, **8**, 1445.

8 C. Giommarelli, V. Zuco, E. Favini, C. Pisano, F. Dal Piaz, N. De Tommasi and F. Zunino, *Cell. Mol. Life Sci.*, 2010, **67**, 995.

9 A. Casbarra, L. Birolo, G. Infusini, F. Dal Piaz, M. Svensson, P. Pucci, C. Svanborg and G. Marino, *Protein Sci.*, 2004, **13**, 1322.

10 Schrödinger, LLC: New York, NY, 2013.

11 M. M. Ali, S. M. Roe, C. K. Vaughan, P. Meyer, B. Panaretou, P. W. Piper, C. Prodromou and L. H. Pearl, *Nature*, 2006, **440**, 1013.

12 R. A. Friesner, R. B. Murphy, M. P. Repasky, L. L. Frye, J. R. Greenwood, T. A. Halgren, P. C. Sanschagrin and D. T. Mainz, *J. Med. Chem.*, 2006, **49**, 6177.

13 W. Humphrey, A. Dalke and K. Schulten, *J. Molec. Graphics*, 1996, **14**, 33.

14 E. Moroni, H. Zhao, B. S. J. Blagg and G. Colombo, *J. Chem. Inf. Model.*, 2014, **54**, 195.

15 M. Yazdanian, S. L. Glynn, J. L. Wright and A. Hawi, Pharm. Res. 1998, 15, 1490; J. D. Irvine, L. Takahashi, K. Lockhart, J. Cheong, J. W. Tolan, H. E. Selick and J. R. Grove, *J. Pharm. Sci.*,1999, **88**, 28; P. Stenberg, U. Norinder, K. Luthman and P. Artursson, *J. Med. Chem*. 2001, **44**, 1927.

16 Caco-2 cells are a model for the gut-blood barrier (QikProp predictions are for non-active transport)

17 C. A. Lipinski, F. Lombardo, B. W. Dominy and P. J. Feeney, *Adv. Drug Delivery Rev.*, 2001, **46**, 3-26.